A Dipole Magnet Model for Compact Synchrotron Light Source

M. Kitamura, H. Yamamoto, H. Tomeoku and N. Maki
Hitachi Research Laboratory, Hitachi, Ltd.
4026 Kuji, Hitachi, Ibaraki 319-12 Japan

Abstract

Compact electron storage rings with superconducting dipole magnets have been developed as the soft X-ray source for the production of LSI (Large Scale Integration). We have manufactured a dipole magnet model with a copper *quasi-cosθ* winding, and measured the field distributions. In this paper, an optimal design technique to determine the cross-sectional coil configuration is described. Results of field measurements and 2-dimensional field calculations are also discussed.

I. INTRODUCTION

Synchrotron radiation, emitted from electrons circulating in the electron storage ring, has been considered as a prospective soft X-ray source for the production of LSI. Designs and constructions of the compact electron storage rings with superconducting dipole magnets, dedicated to this purpose, have been reported during the last several years[1,2,3].

Prior to the design of the superconducting dipole magnet, we have manufactured a normal conducting dipole magnet model of conductor dominated type. The design technique we have used to determine the current density distribution in the vertical cross-sectional plane of the magnet, is based on a combination of the linear programming (LP) and finite element method (FEM), originally proposed by Ishiyama et. al. [4]. Moreover, the Davidon's method has also been used to obtain the final coil configuration. This paper reports the above design techniques and comparison between the measured and calculated magnetic fields in the dipole magnet.

II. OPTIMIZATION PROCEDURE

A. Current Density Distribution

Fig. 1 shows a cross-sectional geometry of the calculation model. We assume that the magnet is axially symmetric with respect to the z-axis. The region of coil is divided into a set of sectoral coil elements and has a gap of given length in the outer coil. Current densities in the coil elements will be taken as unknown variables. Regulated points located appropriately in a region centered at the magnet center line are for restricting magnetic fields. It is also assumed that the iron shield has a constant permeability.

In order to apply LP, we need to express the r and z components of the magnetic flux density B_r, B_z at each regulated point, as a linear combination of the current density vector j (= $(j_1, j_2, \ldots, j_n)$). As long as the second assumption is satisfied, in matrix form this is written as:

$$\begin{pmatrix} B_r \\ B_z \end{pmatrix}_p = [G]_p \vec{j}, \qquad p=1,2, \ldots ,m \tag{1}$$

where

$$[G]_p = \begin{bmatrix} g_{11} & g_{12} & \cdots & g_{1n} \\ g_{21} & g_{22} & \cdots & g_{2n} \end{bmatrix}_p \tag{2}$$

Here n and m are the total numbers of coil elements and regulated points, respectively. G_p is a matrix of the order of 2×n and its matrix elements g_{1i} and g_{2i} are equivalent to the r and z components of the magnetic flux density due to a current of $1A/m^2$ in the ith coil element, respectively. Calculations of the matrix elements of G_p have been performed using the FEM formulation.

Since our design goal is to reduce size and cost of the magnet, we choose the magnetomotive force as the objective function of LP and minimize this. The objective function is given by:

$$Z = \sum_{i=1}^{n} | s_i j_i | \tag{3}$$

where s_i is a cross-sectional area of the ith coil element.

Minimizing the objective function Z, we impose restrictions on both current density in the coil element and magnetic flux density at the regulated point. With respect to the current density, we require:

$$| j_i | \le j_{max}, \qquad i=1,2, \ldots ,n \tag{4}$$

and

$$\sum_{i=1}^{n} s_i j_i = 0 \tag{5}$$

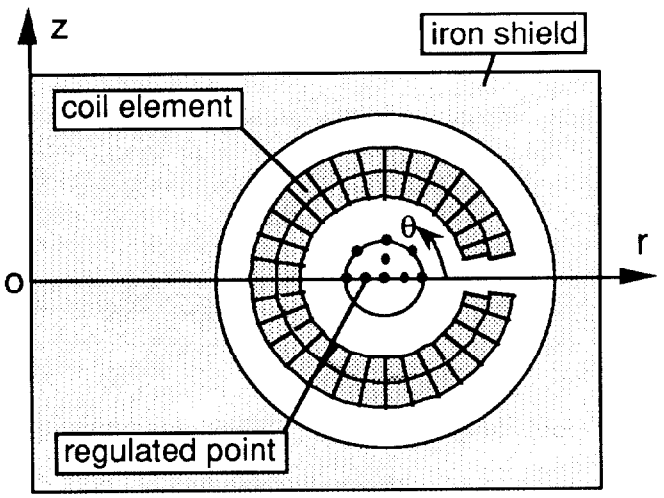

Fig. 1 Calculation model

0-7803-0135-8/91$03.00 ©IEEE

where j_{max} is the given maximum current density. Eq.(5) is imposed for ease of fabrication. Moreover, since the coil region consists of a number of layers as shown in Fig. 1, conditions on current density similar to Eq.(5) may be imposed for each layer.

At each regulated point we also require that the r and z components of the magnetic flux density expressed by Eq.(1) are bounded by:

$$- \Delta B_r \le B_r \le \Delta B_r \tag{6}$$

and

$$B_0 - \Delta B_z \le B_z \le B_0 + \Delta B_z \tag{7}$$

to obtain an uniform dipole field with the good field region of a given size x_0 and field uniformity, where B_0 is the given central magnetic flux density along the z-axis, ΔB_r and ΔB_z are tolerances on the error fields.

Following the numerical procedures explained so far, in principle the current density distribution can be optimized for the given design parameters described above. However, it should be noted that if geometrical parameters for the coil region such as the coil inner radius, number and width of coil layer are not suitably chosen, the LP might not converge or give an answer. In this sense, it is desirable to obtain a suitable initial set of the geometrical parameters before optimizing the problem.

In order to accomplish this, a simpler and faster optimization procedure based on a combination of Biot Savart's law and LP is also used as a tool for the preliminary survey. In this method, each coil element is divided into filamentary conductors and the matrix elements of G_p are calculated by superposing the magnetic fields produced by them. This simple method is a useful tool of the survey over a wide range of various parameters. Further optimizations by a combination of FEM and LP can easily be performed using the initial geometrical parameters obtained.

B. Final Coil Configuration

The procedure to obtain the final cross-sectional coil configuration consists of two steps. Firstly, the cross-sectional shape and number of turns of a key stone type conductor are determined such that the optimized current density distribution obtained in the previous section is approximately realized. Since, in most cases, the coil elements with the maximum current density cluster about certain positions, a set of sectoral coils is obtained in this step as shown in Fig. 3.

The second step adjusts angular positions (θ), depicted in Fig. 1, of each sectoral coil, minimizing the objective function concerning the first two field errors expressed as:

$$\chi = \sum_{n=2}^{3} \left\{ (c_n - \bar{c}_n)\, x_0^{n-1} \right\}^2 \tag{8}$$

by the Davidon's method. Here c_n and $\bar{c}_n$ are multipole expansion coefficients of the fields at the magnet center line, respectively due to the sectoral coils and the optimized current densities in the previous section. This non-linear optimization requires the derivative of c_n with respect to the rotation angle θ of each sectoral coil. On the assumption that the magnet has an infinite bending radius, this is approximately given as[5]:

$$\frac{dc_n}{d\theta} \approx \begin{cases} \dfrac{\mu_0 j_{max}}{\pi(n-2)} \left(\rho_2^{-n+2} - \rho_1^{-n+2}\right)\left(\cos n\theta_2 - \cos n\theta_1\right), & n=1 \\ & n\ge 3 \\ -\dfrac{\mu_0 j_{max}}{\pi} \log\left(\dfrac{\rho_2}{\rho_1}\right)\left(\cos 2\theta_2 - \cos 2\theta_1\right), & n=2 \end{cases} \tag{9}$$

where ρ_1 and ρ_2 are inner and outer radii of the sectoral coil, θ_1 and θ_2 ($\theta_2 > \theta_1$) are side surface angles of the sectoral coil measured from the median plane of the magnet.

III. DIPOLE MAGNET MODEL

Fig. 2 shows the normal conducting dipole magnet model manufactured to verify the optimal design technique described above. This magnet has a 180° sectoral iron shield of 500mm in height, 900mm in outer diameter. The center line of the coil is a 180° arc of 660mm in radius.

The magnetic flux lines and cross-section of the dipole magnet model are shown in Fig. 3. The coil (*quasi-cosθ* con-

Fig. 2 Dipole magnet model

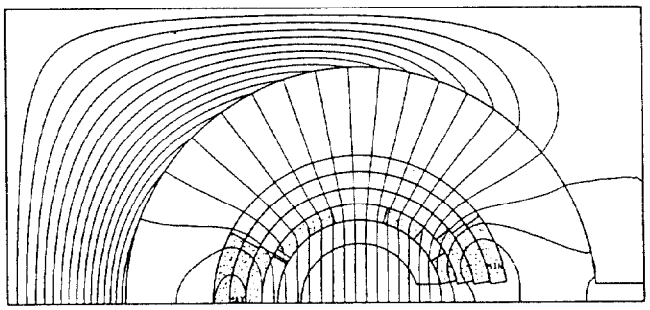

Fig. 3 Magnetic flux lines and cross-section of the dipole magnet model

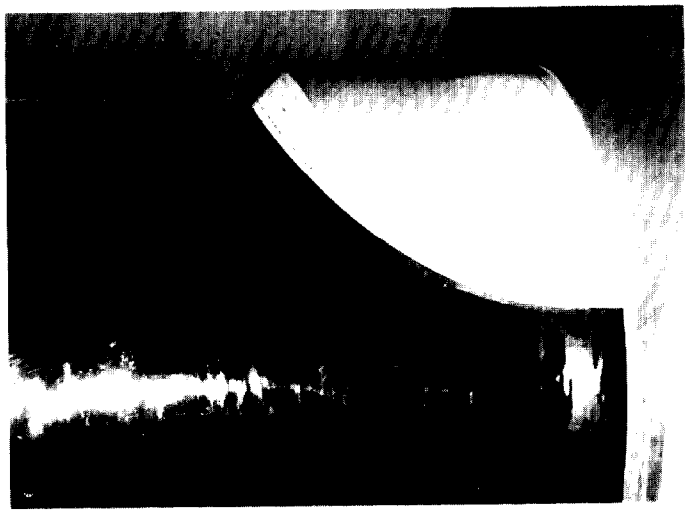

Fig. 4 The end of conductor layer

figuration) consists of two double pancake windings. The key stone angle of the conductor is 1.66°. The inner radius of the coil is 70mm. When optimizing the cross-sectional coil configuration, a central magnetic field of 3T, over-all current density of ~120A/mm^2, 30mm gap in the outer coil, circular good field region of 25mm in radius and field uniformity of less than 5×10^{-4} were required. In Fig. 4, the end of the completed second conductor layer is shown.

To measure the magnetic field distributions, the Hall and NMR probes set on a magnetic measurement fixture capable of 3-dimensional positioning were used .

IV. Measured and Calculated Fields

In Fig. 5, the measured and calculated magnetic fields in the mid-plane and at the magnet center, expressed as field uniformity $\Delta B/B_0$, are plotted as a function of the horizontal coordinate x. The measured field uniformities agree with those calculated by 2-dimensional code within the order of 10^{-4}. Moreover, a good field region of about 50mm wide, which is about 36% of the inner coil diameter, is achieved. This result ensures the validity of the optimization procedure.

Fig. 6 shows the measured vertical magnetic fields normalized by that at the magnet center. The s-axis shown in this figure is a coordinate along the magnet center line. We find that the flat top of the magnetic field extends very close to the end of the magnet and decreases sharply.

V. Conclusion

An optimal design technique using the linear programming and 2-dimensional field calculations by the finite element method has been applied to determine a coil configuration in a 180° sectoral dipole magnet model. Using this model, a good agreement between the measured and calculated field uniformities within the order of 10^{-4} is obtained. Moreover, a designed good field region of about 50mm wide is achieved. This result shows the validity of the design technique.

VI. Acknowledgements

We would like to thank Dr. A. Ishiyama of Waseda University for his suggestions and discussions. The 2-dimensional field calculation code used in this work was written by M. Ito of Hitachi Research Laboratory. The authors also thank T. Yamagiwa and R. Tomita of Hitachi Works for helping with the fabrication of the model.

VII. References

[1] Proceedings of Workshop on Compact Storage Ring Technology: Application to Lithography, BNL 52005, 1986

[2] H. O. Moser, B. Krevet, A. J. Dragt, "Nonlinear Beam Optics with Real Fields in Compact Storage Rings," in Proceedings of the 1987 IEEE Particle Accelerator Conference, Vol.1, pp.458-460

[3] N. Takahashi, "Compact Superconducting SR Ring for X-Ray Lithography," Nucl. Instr. and Meth., Vol.B24/25, pp.425-428, 1987

[4] A. Ishiyama, T. Yokoi, S. Takamori, and T. Onuki, "An Optimal Design Technique for MRI Superconducting Magnet Using Mathematical Programming Method," IEEE Trans. on Magn, Vol.24, No.2, pp.922-925, 1988

[5] K. Halbach, "Fields and First Order Perturbation Effects in Two-Dimensional Conductor Dominated Magnets," Nucl. Instr. and Meth., Vol.78, pp.185-198, 1970

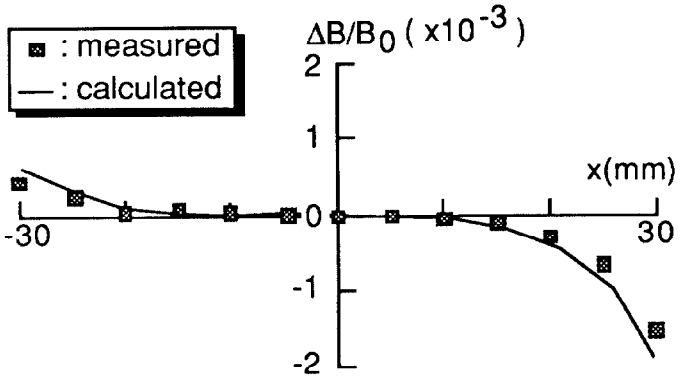

Fig. 5 Field uniformity along the horizontal axis

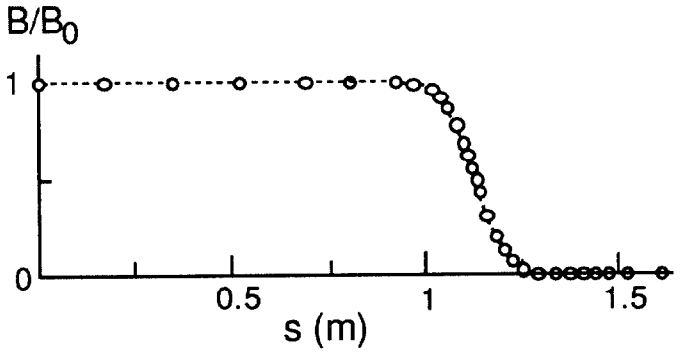

Fig. 6 Vertical field along the magnet center line